

Multi-channel Adaptive Control of Structural Vibration*

Scott D. Sommerfeldt

Applied Research Laboratory, The Pennsylvania State University, P.O. Box 30, State College, PA 16804, USA

*Received: 10 December 1990; revised: 25 July 1991

A multi-channel adaptive control system has been developed for problems involving multi-input multi-output control. The adaptive control system performs both system identification and control in real time, without injecting any additional noise signals into the system. In the present application, the control system has been applied to the problem of minimizing the structural vibration which propagates from a vibrating plate through multiple isolation mounts supporting the plate. The control system was implemented in real time using a Motorola DSP56000ADS signal-processing board. For periodic excitations, the adaptive controller was capable of providing 40 dB attenuation or more at the controlled locations.

Nomenclature

a	convergence parameter for the projection algorithm
b	positive constant to prevent division by 0 in the projection algorithm
$c_{lk}(n)$	transfer function relating the reference input signal to $d_l(n)$
$d_l(n)$	signal at l th error sensor with no control applied
$\mathbf{d}(n)$	vector comprised of the L signals, $d_l(n)$
$e_l(n)$	error signal from the l th error sensor
$\mathbf{e}(n)$	vector comprised of the L error signals, $e_l(n)$
$E\{\}$	expected value operator
$H_{lm}(n)$	transfer function from the m th control signal to the l th error signal
$h_{lmj}(n)$	j th coefficient of $H_{lm}(n)$
$\mathbf{H}_l(n)$	vector comprised of the M transfer functions, $H_{lm}(n)$
h_{max}	largest value of the transfer function coefficients, $h_{lmj}(n)$
I	total number of control filter coefficients
J	total number of coefficients in the transfer function $H_{lm}(n)$
J_c	performance function to be minimized by the adaptive controller
K	total number of coefficients for the $c_{lk}(n)$
L	total number of error sensors
M	total number of control actuators
n	discrete time index
$r_{lm}(n)$	filtered reference input used to adapt the control filter
$\mathbf{r}(n)$	vector comprised of the M filtered input signals, $r_{lm}(n)$
$\mathbf{R}(n)$	matrix comprised of the L vectors, $\mathbf{r}_l(n)$
$R_{xx}(\tau)$	autocorrelation function of the reference input signal, $x(n)$
$w_{mi}(n)$	i th control filter coefficient for the m th control signal
$W_m(n)$	control filter transfer function for the m th control signal

$\mathbf{W}(n)$	vector comprised of the M control filter transfer functions, $W_m(n)$
$x(n)$	reference input signal
$y_m(n)$	control signal for the m th actuator
$\mathbf{Y}(n)$	vector comprised of the M control signals, $y_m(n)$
$\Theta_l(n)$	vector consisting of $\mathbf{H}_l(n)$ augmented with $c_{lk}(n)$
$\hat{\Theta}_l(n)$	estimate of $\Theta_l(n)$ at time n
μ	convergence parameter for the control algorithm
$\Phi(n)$	vector consisting of $\mathbf{Y}(n)$ augmented with $x(n)$

Introduction

The development of faster and more powerful digital signal processing boards in recent years has been accompanied by a greatly increased interest in active noise and vibration control. Along with this increased interest has come significant progress in developing an increased understanding of active control. Active control involves the use of secondary sources which are applied to the system to control the disturbance created by the primary source. The degree of coupling which exists between secondary sources and the primary source depends on the spacing between the primary and secondary sources, and determines the performance which can be achieved from an active control system. If the sources are located in such a way that they are closely coupled, the primary and secondary sources will interact with each other, making it possible to achieve a global reduction of the energy in the field.¹ The effect of this

interaction is that the impedance seen by each source is altered. If the secondary source velocity is out of phase with the force (or pressure, in a fluid) at the secondary source location, the secondary source will produce negative power (i.e., it is an energy sink). This phenomenon also has the effect of altering the impedance seen by the primary source, thereby altering its power output as well. On the other hand, if the secondary sources are not coupled to the primary source, it is still possible to minimize the disturbance at some desired location, but at the expense of increasing the total power in the field.

To achieve successful results using active control, one must be able to accurately determine both the amplitude and phase of the control signal necessary to minimize the disturbance. If the parameters of the system are known with sufficient accuracy, it is possible to achieve the desired goal using a fixed controller. However, typically the parameters may be difficult to determine accurately, or the parameters may change in time. In such cases, a fixed controller can be expected to give sub-optimal control. Adaptive control provides an attractive means for implementing active control, since the control algorithm will adapt in real-time and converge to the solution for the optimal control filter. In addition, it is not critical to have highly accurate *a priori* estimates of the parameters of the system.

Much of the research reported on adaptive control involves the control of sound propagating in a fluid (i.e., air), or of sound radiated from a vibrating structure. These applications include the minimization of noise propagating in a duct, the minimization of the energy density in an enclosure, and the minimization of sound radiated from a panel.²⁻⁷ The majority of applications reported to date have involved a single quantity which is minimized by a single control source. Thus, the control system can be characterized as a single-input/single-output controller.

There have been a number of active vibration control schemes reported in the literature. Active vibration control offers considerable potential in controlling the vibration of a structure for such purposes as minimizing fatigue of the structure or minimizing radiation from the structure into an acoustic medium. Until recently, much of the research reported on active vibration control was nonadaptive in nature, generally based on some form of feedback control law.⁸⁻¹³ However, there are advantages to having an adaptive system for active vibration control, just as for active noise control. Recently, there has been increasing interest in developing adaptive active vibration control systems, which have generally been based on some form of feedforward control law. White and Cooper developed a control system for isolation mounts using a frequency domain approach which could be slowly adapted.¹⁴ More recently, adaptive control systems have been developed which are capable of adapting on much shorter time scales.¹⁵⁻¹⁶

A number of applications for active vibration control can be formulated as single-input/single-output control problems, analogous to the duct problem for active noise control. Previous work was reported regarding the minimization of the vibration transmitted through an isolation mount, which represents a single-input/single-output control problem.¹⁷ This paper considers an extension of this work to investigate adaptive control of vibrating plates using multiple control actuators. The adap-

tive controller developed is based on the least-mean-squares (LMS) algorithm, developed by Widrow, *et al.*, for use in signal processing applications.¹⁸⁻¹⁹ The adaptive algorithm can be characterized as a single-input/multi-output control algorithm, and differs from previously reported schemes in that the controller performs both system identification and control in real-time, without the necessity of introducing any added noise signal.

Development of the Multi-channel Algorithm

In developing the adaptive controller, a model-reference approach has been adopted, whereby the controller converges so as to have the same input/output characteristics as the system to be controlled. In the development of the LMS algorithm, the output of the LMS filter is assumed to be the convolution of the input data sequence to the filter with the LMS filter coefficients. As such, the LMS algorithm can be described as an adaptive finite impulse response (FIR) filter. If this assumption is extended to a multi-channel algorithm, with M outputs, the output of the m th LMS filter $y_m(n)$ can be represented as

$$y_m(n) = \sum_{i=0}^{I-1} w_{mi}(n)x(n-i) , \quad (1)$$

where $x(n)$ is the input data sequence, $w_{mi}(n)$ represent the (possibly) time-varying LMS filter coefficients, n represents a discrete time index, and I represents the number of LMS coefficients. These control signals are then used to drive the M control actuators in such a way as to minimize some selected performance function, J_e . For the development in this paper, the performance function is obtained as the sum of the squared outputs from L error sensors, which measure the vibration of the plate. Thus, J_e can be written as

$$J_e = \sum_{l=1}^L e_l^2(n) , \quad (2)$$

where $e_l(n)$ is the l th error signal which results from the response of the plate to the primary excitation and all M control actuators. If the expected value of the sum in Eq. (2) is minimized, the optimal Wiener solution results. Since this expected value is often not available, the LMS algorithm converges to this solution using a gradient descent method and an instantaneous estimate of the gradient of the performance function. This corresponds to using a performance function as given in Eq. (2). By using the sum of the squared errors, a quadratic performance function is obtained, which is characterized by a global minimum, corresponding to the optimal control solution.

It was mentioned that each error signal is affected by each of the control actuators. In active noise or vibration control, a transfer function exists which relates the m th control output, $y_m(n)$, to the response at the l th error sensor due to that control

output. This transfer function will be referred to as the “ l th control path transfer function,” and will be denoted by $H_{lm}(n)$. In the context of the present problem, this transfer function represents the D/A converter, the m th control actuator response function, the system (plate) transfer function between the m th control actuator and the l th error sensor, and the l th error sensor response function. Since there are multiple actuators and error sensors, there will also be multiple control path transfer functions. This is shown schematically in Fig. 1, for the case of two control actuators and two error sensors. For the control scheme developed in this study, it is assumed that the control path transfer functions can be modelled with sufficient accuracy by FIR filters. Using this assumption, the response of the l th error sensor can be represented by

$$\begin{aligned} e_l(n) &= d_l(n) + \sum_{m=1}^M \sum_{j=0}^{J-1} h_{lmj}(n) y_m(n-j) \\ &= d_l(n) + \sum_{m=1}^M \sum_{j=0}^{J-1} \sum_{i=0}^{I-1} h_{lmj}(n) w_{mi}(n-j) x(n-j-i) . \end{aligned} \quad (3)$$

In this equation, $d_l(n)$ is the response to the primary excitation at the l th error sensor, which represents the disturbance to be minimized, and the $h_{lmj}(n)$ represent the lm th control path transfer function, $H_{lm}(n)$, which has J coefficients and may be time-varying.

From Eq. (3), it can be seen that two transfer functions must be determined to obtain optimal control. Determining the proper values of the $h_{lmj}(n)$ represents a problem in system identification, while determining the proper values of the $w_{mi}(n)$ represents the control problem. If the system to be controlled is truly stationary, it is possible to determine the proper values for one or the other (or both) of these two transfer functions off-line, from which the optimal controller could be determined and implemented. However, if the system is time-varying, the performance of the controller will be degraded as the off-line estimates become less accurate. If the system parameters change sufficiently, it is even possible for the control system to become unstable. Thus, a means of determining the control path transfer functions and the LMS control transfer functions adaptively would be desirable. It will be shown below that both of these transfer functions can be determined adaptively in real-time, without the need for any additional noise signals.

System Identification. This section outlines the procedure used for adaptively estimating the proper values for the control path transfer function coefficients, $h_{lmj}(n)$. The development is simplified through the use of several vector definitions. Defining

$$\mathbf{H}_l^T(n) \equiv [h_{l10}(n) \ h_{l11}(n) \dots h_{l1(J-1)}(n) \mid h_{l20}(n) \dots h_{l2(J-1)}(n) \mid \dots \mid h_{lM0}(n) \dots h_{lM(J-1)}(n)] \quad (4)$$

and

$$\mathbf{Y}^T(n) \equiv [y_1(n) \ y_1(n-1) \dots y_1(n-J+1) \mid y_2(n) \dots y_2(n-J+1) \mid \dots \mid y_M(n) \dots y_M(n-J+1)] , \quad (5)$$

allows the error signal to be written as

$$e_l(n) = d_l(n) + \mathbf{H}_l^T(n) \mathbf{Y}(n) . \quad (6)$$

In the development of the LMS algorithm, it is assumed that the input to the LMS filter, $x(n)$, is correlated in some way with the signal to be canceled, $d_l(n)$. Using this assumption, it is possible to relate $x(n)$ to $d_l(n)$ by means of a transfer function, where it will again be assumed that this relationship can be sufficiently and accurately modelled using a FIR filter. This relationship will be represented by

$$d_l(n) = \sum_{k=0}^{K-1} c_{lk}(n) x(n-k) . \quad (7)$$

If the vectors defined in Eqs. (4) and (5) are now augmented, according to

$$\Theta_l^T(n) \equiv [h_{l10}(n) \dots h_{lM(J-1)}(n) \mid c_{l0}(n) \dots c_{l(K-1)}(n)] \quad (8)$$

and

$$\Phi^T(n) \equiv [y_1(n) \dots y_M(n-J+1) \mid x(n) \ x(n-1) \dots x(n-K+1)] , \quad (9)$$

it is possible to represent the l th error signal in the simple form

$$e_l(n) = \Theta_l^T(n) \Phi(n) . \quad (10)$$

In the above expression for the l th error signal, it will be noted that measured values of $e_l(n)$ are available, as are all of the values in $\Phi(n)$, either as measured input signals or calculated control signals. Thus, the only unknown values are the desired coefficients in the vector $\Theta_l(n)$. There are a number of adaptive estimation algorithms available for determining the coefficients in the vector $\Theta_l(n)$. In the present work, the projection algorithm (sometimes referred to as the normalized LMS algorithm in the literature) was used.²⁰ For the projection algorithm, if the estimate of $\Theta_l(n)$ is denoted by $\hat{\Theta}_l(n)$, the coefficients are updated according to

$$\hat{\Theta}_l(n+1) = \hat{\Theta}_l(n) + \frac{a\Phi(n)}{b + \Phi^T(n)\Phi(n)} [e_l(n) - \hat{\Theta}_l(n) \Phi(n)] , \quad (11)$$

where b is a constant greater than 0 to prevent division by zero, $0 < a < 2$ to ensure convergence of the algorithm, $e_l(n)$ is the measured error signal, and $\hat{\Theta}_l^T(n)\Phi(n)$ represents the estimated error signal.

The projection algorithm will converge to a solution which minimizes the difference between the measured error at the l th error sensor and the estimated error at that sensor. Whether this solution converges to a model of the true system parameters or not depends on the characteristics of the input signal.²¹

However, in the context of active vibration control, the important property is whether the solution converges to give the proper input/output relationships for the frequencies present. The projection algorithm will do this, even if the resulting solution does not necessarily represent the actual parameters of the system.²⁰ Furthermore, the only information which is used to obtain the solution are those signals which are naturally available from the system. This is in contrast to other systems which are either nonadaptive, or introduce additional excitation signals into the system to obtain the proper model.^{22,23}

System Control. To develop the multi-channel algorithm used to determine the optimal control signals, it is desired that the performance function given by Eq. (2) be minimized. The approach adopted here has been developed previously, and is presented here briefly for the sake of completeness.²⁴ To obtain the desired result, it is useful to consider the case where the LMS filter coefficients, w_{mi} , are time invariant. This is approximately true when the solution for w_{mi} is close to the optimal solution. As Elliott, *et al.*, discuss, assuming time invariance is equivalent to assuming the filter coefficients w_{mi} are only slowly varying relative to the timescale of the response of the system to be controlled.²⁴ Using this assumption allows Eq. (3) to be rearranged as

$$e_l(n) = d_l(n) + \sum_{m=1}^M \sum_{i=0}^{I-1} w_{mi} \sum_{j=0}^{J-1} h_{lmj}(n)x(n-j-i) . \quad (12)$$

The form of this equation corresponds to inverting the order of the two transfer functions, W_m and H_{lm} . The last term in Eq. (12) can be seen to correspond to the input signal being filtered by the transfer function, H_{lm} . Thus, to simplify the equation, define

$$r_{lm}(n-i) \equiv \sum_{j=0}^{J-1} h_{lmj}(n)x(n-j-i) , \quad (13)$$

along with the vectors

$$\mathbf{W}^T \equiv [w_{10}w_{11}\dots w_{1(I-1)} | w_{20}\dots w_{2(I-1)} | \dots | w_{M0}\dots w_{M(I-1)}] , \quad (14)$$

and

$$\mathbf{r}_l^T(n) \equiv [r_{l1}(n)r_{l1}(n-1)\dots r_{l1}(n-I+1) | r_{l2}(n)\dots r_{l2}(n-I+1) | \dots | r_{lM}(n)\dots r_{lM}(n-I+1)] . \quad (15)$$

With these definitions, the l th error signal can be expressed as

$$e_l(n) = d_l(n) + \mathbf{r}_l^T(n)\mathbf{W} . \quad (16)$$

For the adaptive control algorithm, it is desired to minimize the signals from all L error sensors. To determine the sum of the squared errors required for the performance function given

in Eq. (2), define the $L \times 1$ vectors

$$\mathbf{e}^T(n) \equiv [e_1(n)e_2(n)\dots e_L(n)] , \quad (17)$$

$$\mathbf{d}^T(n) \equiv [d_1(n)d_2(n)\dots d_L(n)] , \quad (18)$$

and the $MI \times L$ matrix

$$\mathbf{R}(n) \equiv [\mathbf{r}_1(n)\mathbf{r}_2(n)\dots \mathbf{r}_L(n)] . \quad (19)$$

With this notation, the error vector, $\mathbf{e}(t)$, can be written as

$$\mathbf{e}(n) = \mathbf{d}(n) + \mathbf{R}^T(n)\mathbf{W} , \quad (20)$$

and the performance function can be expressed as

$$J_c = \sum_{l=1}^L e_l^2(n) = \mathbf{e}^T(n)\mathbf{e}(n) . \quad (21)$$

The expression for the error vector in Eq. (20) can be used in Eq. (21) to reveal the quadratic dependence of the performance function on the LMS filter vector, \mathbf{W} .

$$J_c = \mathbf{d}^T(n)\mathbf{d}(n) + 2\mathbf{d}^T(n)\mathbf{R}^T(n)\mathbf{W} + \mathbf{W}^T\mathbf{R}(n)\mathbf{R}^T(n)\mathbf{W} . \quad (22)$$

The LMS algorithm is a gradient descent algorithm. Thus, to determine the proper form of the control algorithm, the gradient of Eq. (22) with respect to \mathbf{W} must be obtained. The estimate of the LMS filter is then updated according to the negative gradient until it converges to the optimal solution where the gradient is equal to zero. The result of this process yields an update for the LMS filter given by

$$\mathbf{W}(n+1) = \mathbf{W}(n) - \mu\mathbf{R}(n)\mathbf{e}(n) , \quad (23)$$

where μ is a convergence parameter greater than zero, chosen to maintain stability. Eq. (23) can be viewed as a multi-channel generalization of the filtered- x LMS algorithm developed by Widrow and Stearns.²⁵ It can be shown that the algorithm described by Eq. (23) is stable for values of μ in the range $0 < \mu < 2/\lambda_{\max}$, where λ_{\max} is the largest eigenvalue of the "filtered autocorrelation" matrix, given by $E\{\mathbf{R}(n)\mathbf{R}^T(n)\}$.²⁶ In practice, the eigenvalues of this matrix are seldom known. A more restricted, but practical, convergence criterion based on the average input power can be developed, with the resulting criterion being given by:²⁷

$$0 < \mu < \frac{2}{h_{\max}^2 [L \cdot M \cdot I \cdot J^2] R_{xx}(0)} , \quad (24)$$

where $R_{xx}(0)$ represents the average power of the input signal, $x(n)$, and h_{\max} represents the largest value the h_{lmj} may assume. A brief derivation of this result, along with the assumptions associated with it, is given in Appendix A. An important result concerning multi-channel control can be seen by examining Eq. (24). The denominator of the upper limit for the conver-

gence parameter is proportional to both the number of error sensors, L , and the number of control actuators, M . Thus, as additional control actuators and/or error sensors are added to the control system, the algorithm must converge at a slower rate, all else remaining equal. This is due to the time constant of adaptation being inversely proportional to the convergence parameter.²⁸ If the number of error sensors equals the number of control actuators, then the convergence speed rapidly becomes severely limited as the number of channels is increased, which means that a system with a large number of channels will not be able to converge nearly as fast as a corresponding single-channel system.

System Feedback. The control system described above, with the system identification algorithm for identifying the \mathbf{H}_l and the system control algorithm for determining the W_m , can be expected to be stable and converge to the optimal solution if the convergence parameters are selected properly, based on the principle of certainty equivalence control.²⁹ This conclusion is based on two conditions: (a) the identification algorithm converges on a faster time scale than the control algorithm, so that a good model of the system is available as soon as possible; and (b) the input signal to the control system $x(n)$ remains bounded, such that the FIR filter output also remains bounded. For a structure or an acoustic system, not only do the control actuators produce a response at the error sensors, but if the input sensor is sensitive to the output of the control actuators, they also produce a response at the input sensor. If the magnitude of the gain of this feedback loop becomes greater than unity for some frequency, the control system will become unstable at that frequency.

There are several ways of compensating for this potential problem. The simplest solution, which is practical in some cases, is to make the input sensor for the control system insensitive to feedback from the control actuators. An example of this would be control of a rotating shaft, where the input signal could be obtained from a tachometer on the shaft which measures the frequency of rotation of the shaft. This signal will not change when the control actuators are operating, resulting in a stable control system.

If the input sensor is sensitive to feedback from the control actuators, there must be some sort of compensation to remove the effects of the feedback. One approach to compensate for the feedback involves the use of an infinite-impulse-response (IIR) transfer function in place of the finite-impulse-response (FIR) transfer function used for the LMS algorithm. The RLMS algorithm used by Eriksson, *et al.*, represents such an approach.²³ By using an IIR transfer function, the denominator of the transfer function models the feedback path from the control actuator to the input sensor.

Another approach, developed by Warnaka, *et al.*, introduces additional compensation filters to model the feedback.²² The compensation filters are determined adaptively in an *a priori* setup procedure, so as to model the transfer function of the feedback paths. The filters are then fixed for real-time operation. To compensate for the feedback, the control signals sent to the actuators are also passed through the compensation fil-

ters, thereby modelling the feedback through the structure. The output of the compensation filters is then subtracted from the measured signal at the input sensor, and this result is used as an error signal to adaptively remove the feedback effects. This approach was used for some of the results presented in the following sections.

Implementation of the Control System. For the results presented in this paper, the procedures outlined previously for system identification and control were combined to obtain an adaptive control system which is capable of achieving multi-channel control. This process is shown schematically in Fig. 1. The controller is based on gradient descent techniques, with the various transfer functions being updated each sample period. There are four operations which are performed each sample period, given by Eqs. (1), (11), (13), and (23). For clarity, those equations are reproduced here.

$$y_m(n) = \sum_{i=0}^{L-1} w_{mi}(n) x(n-i); m = 1, 2, \dots, M \quad (1)$$

$$\hat{\Theta}_l(n+1) = \hat{\Theta}_l(n) + \frac{a\Phi(n)}{b + \Phi^T(n)\Phi(n)} [e_l(n) - \hat{\Theta}_l^T(n)\Phi(n)]; l=1, \dots, L \quad (11)$$

$$r_{lm}(n-i) \equiv \sum_{j=0}^{L-1} h_{lmj}(n)x(n-j-i); l=1, 2, \dots, L, m=1, 2, \dots, M \quad (13)$$

$$w_{mi}(n+1) = w_{mi}(n) - \mu \sum_{l=1}^L e_l(n)r_{lm}(n-i); m = 1, 2, \dots, M \quad (23)$$

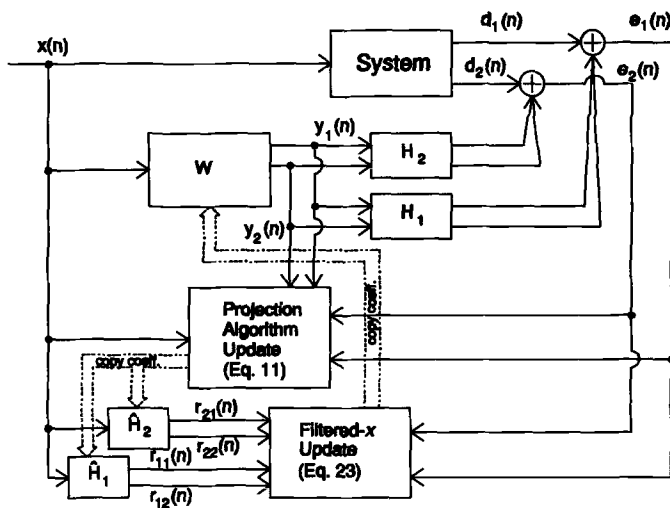


Figure 1. Block diagram of multi-channel control system for the case of two control actuators and two error sensors

In the last equation, Eq. (23) has been reproduced for a single component of the LMS transfer function vector to explicitly show the operations involved.

For implementation, it is necessary to initialize the $\hat{\Theta}_l$ transfer functions to have a nonzero value to obtain proper performance of the projection algorithm. In this work, no attempt was made to start from an initial estimate of the actual transfer functions of the system. Thus, all coefficients in the $\hat{\Theta}_l$ transfer functions were initialized to have a value of 0.0625 (hex 080000), and all the w_{mi} coefficients were initialized to a value of 0.

Some of the experiments were performed using an external signal as the input to the LMS filters, so as to eliminate any feedback through the system from the control actuators. However, some of the experiments were also performed using an input signal from a sensor located on the structure, and therefore sensitive to system feedback. For these experiments, the compensation scheme described previously was used to remove the feedback effects from the input signal before sending the input to the LMS filters.

Experimental Apparatus

The control system described previously was used to control vibration transmission associated with an aluminum plate in transverse vibration, supported by isolation mounts, located near each of the four corners of the plate (Figure 2). The dimensions of the plate were $0.6096\text{m} \times 0.4064\text{m} \times 0.0127\text{m}$, and the stiffness of each isolation mount was 2767 N/m . The isolation mounts were attached to a foundation, assumed to be rigid. The objective of the control was to minimize the vibration at each of the mount locations, thereby minimizing the transmission of forces through the mounts to the foundation.

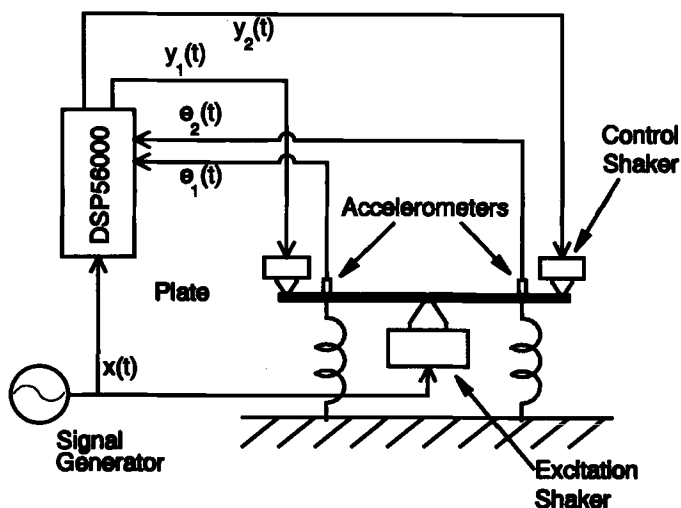


Figure 2. Schematic diagram of vibrating plate with isolation mounts and the associated control system shown here for two channels

To accomplish this objective, "error" sensors were placed at each of the isolation mount locations, to monitor the vibration levels at those locations.

The performance function consisted of the sum of the squared error sensor signals. To control the structure, Wilcoxon F3 electrodynamic shakers were attached to each corner of the plate. These locations were chosen to allow the shakers to efficiently couple into the various modes which could be excited in the plate. To excite the plate, a larger Wilcoxon F4 shaker was attached to the plate near the center of the plate. The excitation shaker was driven from a signal generator which could excite a single frequency, multiple frequencies, or broadband signals.

The control system equations described previously were implemented in real-time using the Motorola DSP56000ADS signal processing board. The error signals required were obtained by means of PCB 303A11 accelerometers. The input signal was taken from the signal generator driving the primary excitation source, for the case of no feedback path, and taken from a PCB 303A11 accelerometer mounted on the plate near the primary source for the case of feedback compensation. The input and error signals were passed through Ithaco Model 257A low-pass filters, and digitized by means of Ariel ADC56000 I/O boards, which interface with the Motorola DSP56000ADS. The control signals determined from the control equations were passed out the Ariel ADC56000, through the Ithaco filters, and amplified to drive the Wilcoxon control shakers.

For the results presented here, the sampling frequency was 2000 Hz. During each sample period, the input signal and error signals were measured, the control signals calculated, the control path transfer function estimations updated, and the LMS control filter updated.

Experimental Results

The control system described previously was implemented using one, two, and four active control sources to control a vibrating plate. This section will present some experimental results obtained for various control configurations. The controller was first tested to determine the convergence properties as a function of the number of channels used in the controller. Figures 3-5 show time-domain results for the convergence of the error signals for one, two, and four active control sources, respectively. For all three cases, the same error signal is shown, and corresponds to an accelerometer in the same corner as a control source which is active. The excitation frequency used was 170 Hz, which corresponds to the bending mode resonance of the (3,1) mode of the plate used. Here, (3,1) indicates 2 nodal lines in the long dimension of the plate, and 0 nodal lines in the short dimension of the plate. It should also be mentioned that in the case of one- and two-channel control, the remaining control actuators were still mounted on the plate so as to keep the mass-loading effects constant in all cases, but were not driven actively.

From Fig. 3, it can be seen that the control system converged to its final solution in approximately 0.6 sec. The convergence is dependent upon the convergence parameter, μ , in

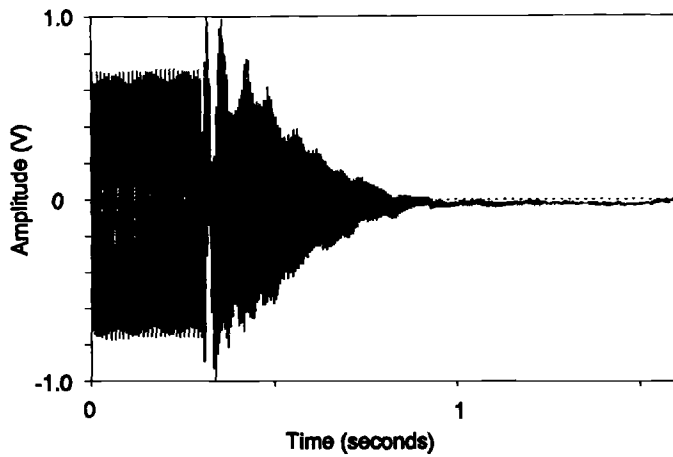


Figure 3. Time history of the error signal for one-channel control and a 170 Hz excitation signal. Control begins at about 0.3 second

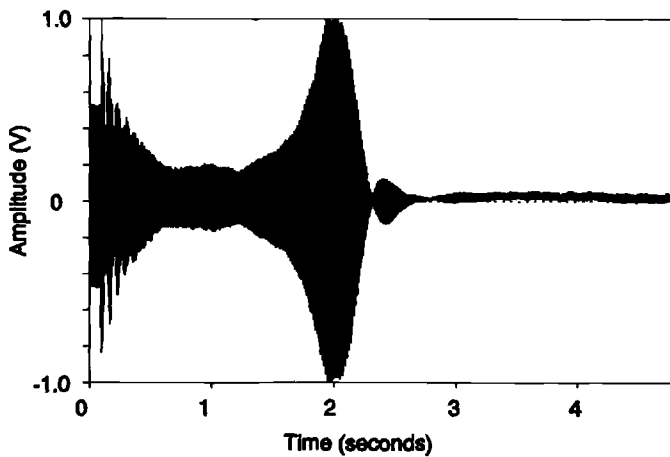


Figure 4. Time history of the error signal for two-channel control and a 170 Hz excitation signal. Control begins at about 0.1 second. The error signal shown is from the same sensor as for Fig. 3

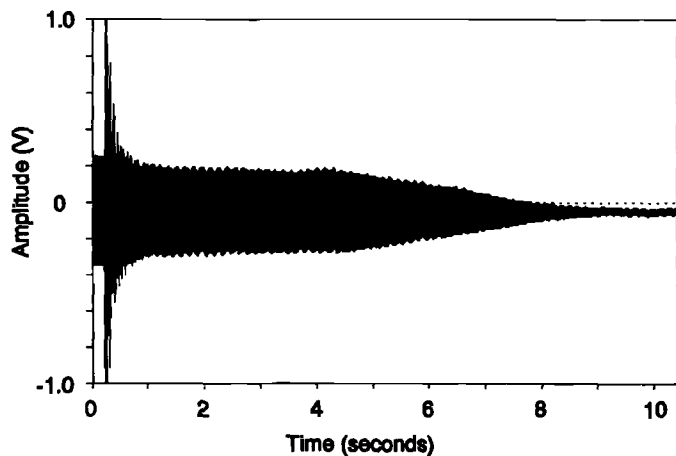


Figure 5. Time history of the error signal for four-channel control and a 170 Hz excitation signal. Control begins at about 0.2 second. The error signal shown is from the same sensor as for Fig. 3

Eq. (23), which was determined in all cases according to Eq. (24). In determining the convergence parameter, the algorithm multiplies the maximum allowable convergence parameter by some constant between zero and one. For Figs. 3-5, this constant was set to a value of 30 and not changed. Thus, the convergence parameter would be expected to decrease (and the convergence time to increase) approximately according to the square of the number of control channels used. (For these results, the number of error sensors used, L , was equal to the number of control actuators used, M .)

This conclusion is based on the assumption that the control system has accurate system identification estimates available from the start. To approximate this condition, the system identification algorithm was set to converge considerably faster (by a factor of about 8) than the control algorithm for these results. While accurate system identification is obviously not available at the initial onset of control, the results seem to indicate that this is not a bad approximation when the system identification algorithm converges faster than the control algorithm. For two-channel control, the convergence time was approximately 2.7 seconds (Fig. 4), and for four-channel control, the convergence time can be seen to be approximately 9 sec. (Fig. 5). The trend apparent here is consistent with what one would predict using Eq. (24), suggesting that Eq. (24) provides a reasonable estimate of the relative convergence time for the various cases. The implication of these results is that the larger the number of channels used, the slower the control system must converge to its final solution. In particular, for the two- and four-channel cases, it was found that even when the convergence was pushed to the stability limits, the system could not converge as fast as for a nominal one-channel case.

Another feature of this control scheme can be seen in Fig. 4. In this case, before converging to the final solution, the error signal diverges to some extent before the control system converges to the final solution which minimizes the performance function. This phenomenon was not always observed, but was not uncommon. This is thought to be associated with the fact that the control scheme actually involves two simultaneous adaptive processes associated with the system identification problem and the system control problem. These two adaptive processes interact with each other in the convergence process, but do not seem to cause any instability as long as the convergence parameters are chosen to lie in the stable regime. It was found experimentally that this effect could be minimized by reducing the convergence speed of the control algorithm, and completely eliminated by allowing the estimation algorithm to converge close to its solution before turning on the control algorithm. It should be mentioned again that no attempt was made in these results to obtain an initial estimate of the correct transfer functions. One aspect of the current research is to fully investigate the interaction between the two algorithms, so as to gain a greater understanding of the properties of the control system, including stability and convergence.

It is often easier to visualize the performance of the control system when the results are presented in the frequency domain. Thus, the remaining results will present the frequency spectra of the error sensor signals for various control configura-

tions. Figure 6 shows the results for the one-channel case, corresponding to the controller driving a single control actuator to minimize the vibration at the error sensor closest to the control actuator, while ignoring the response at other error sensors. For reference, corner 1 is used to refer to the error sensor near the first corner of the plate. The numbering scheme is such that corners 1 and 3 are opposite each other, as are corners 2 and 4. Again, the excitation frequency is 170 Hz. For the one-channel case, the controller successfully attenuated the vibration at corner 1 by about 62 dB, but had only minimal effect at corners 2 and 4 and attenuated corner 3 by only 11 dB.

Figure 7 shows similar results for the two-channel case, with active control actuators located at corners 1 and 3; i.e., at opposite corners of the plate. For the two-channel case, the vibration at corners 1 and 3 was attenuated by 45 dB and 71 dB, respectively, while corners 2 and 4 were again largely unaffected.

In fact, in this case, the levels at corners 2 and 4 actually increased by about 1 dB when the control was applied. It should be mentioned that it was found that operating the control shakers introduced low-level 60 Hz noise into the signals measured, which can be recognized as the additional peaks in the controlled spectra.

Figure 8 shows the corresponding results for the four-channel case, with active control actuators at all four corners of the plate. In this case, all four corners were successfully attenuated by about 45 dB, except for corner 4, which was only attenuated by about 26 dB. The reason for this discrepancy is not readily understood. However, it may be associated with the fact that the convergence parameter of each channel was set to be somewhat different to prevent fighting between channels as the system converges. The convergence of channel 4 was set to be the slowest, which may result in the reduced attenuation at

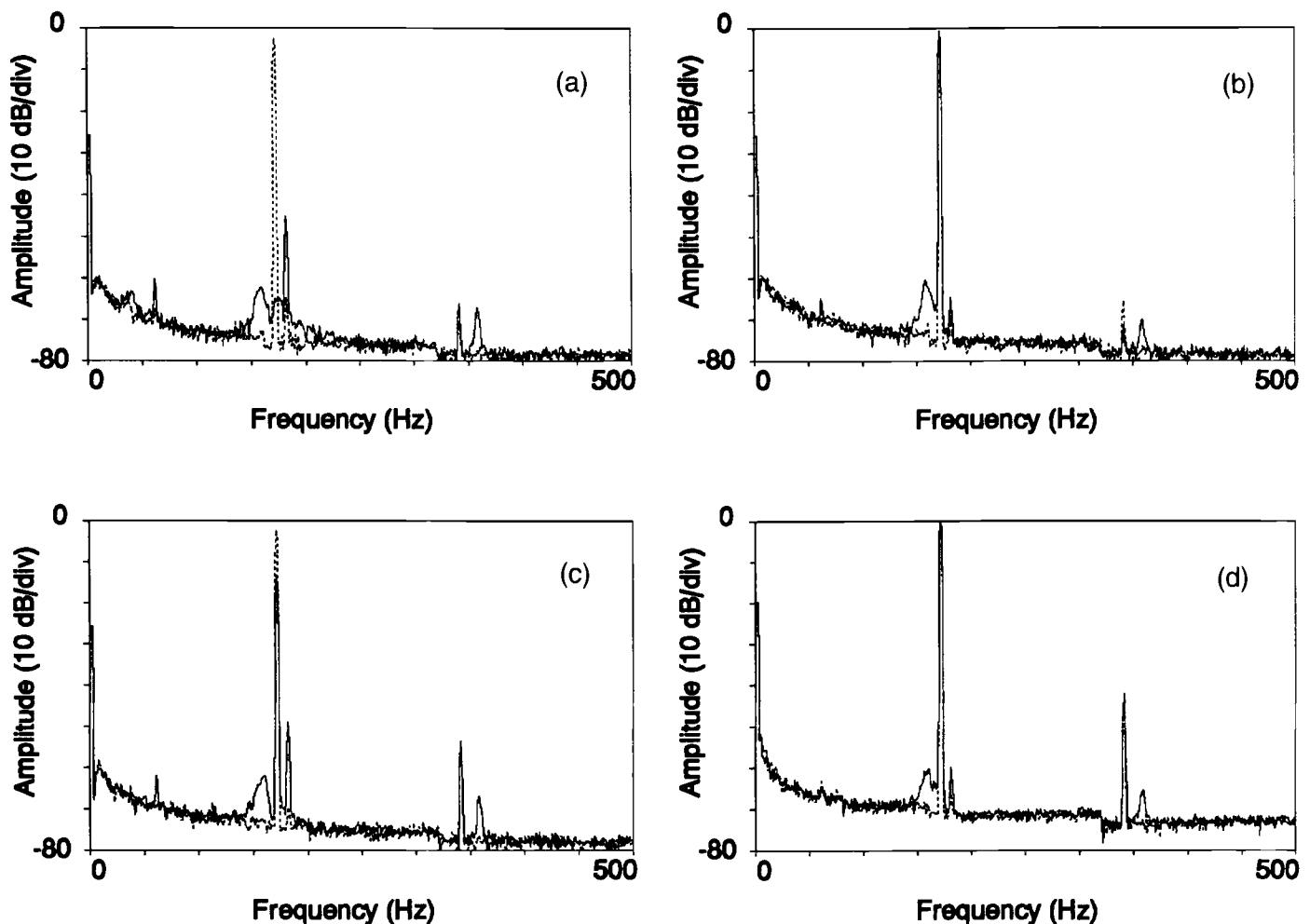


Figure 6. Error signal spectrum for one-channel control. Without control, dashed line; with control, solid line.

(a) corner 1
(b) corner 2

(c) corner 3
(d) corner 4

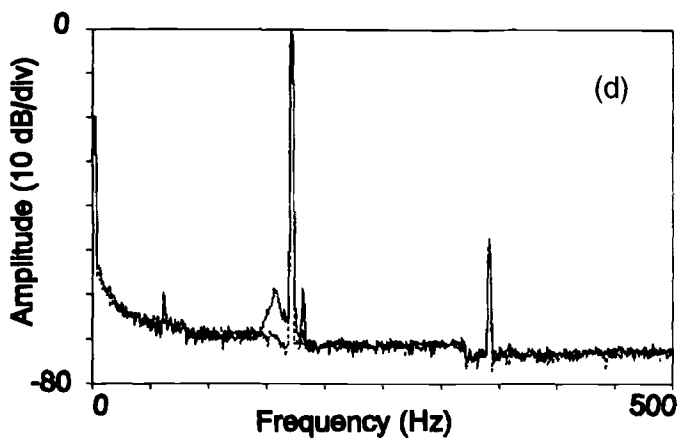
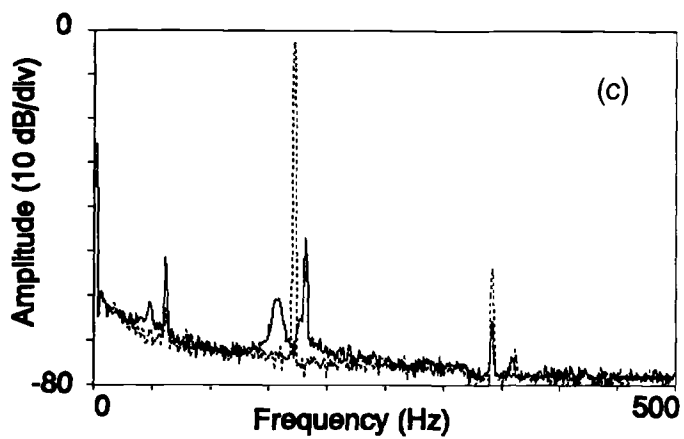
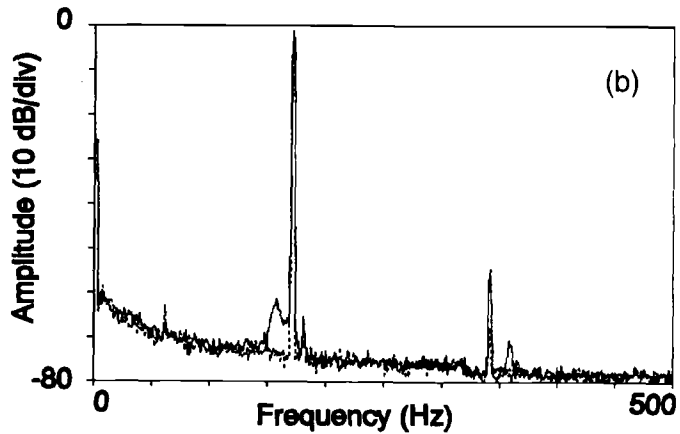
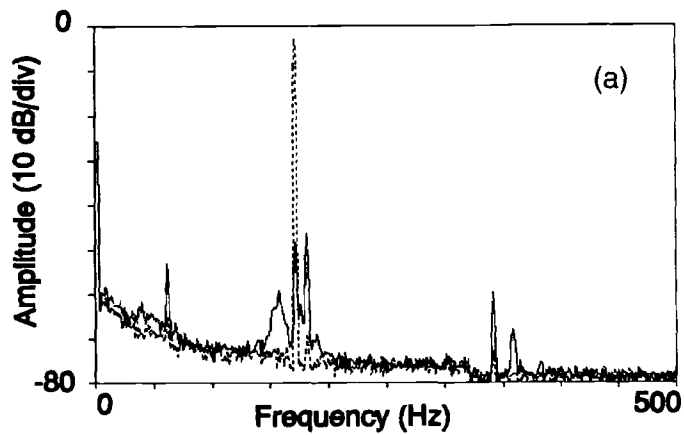


Figure 7. Error signal spectrum for two-channel control. Without control, dashed line; with control, solid line.

(a) corner 1 (c) corner 3
(b) corner 2 (d) corner 4

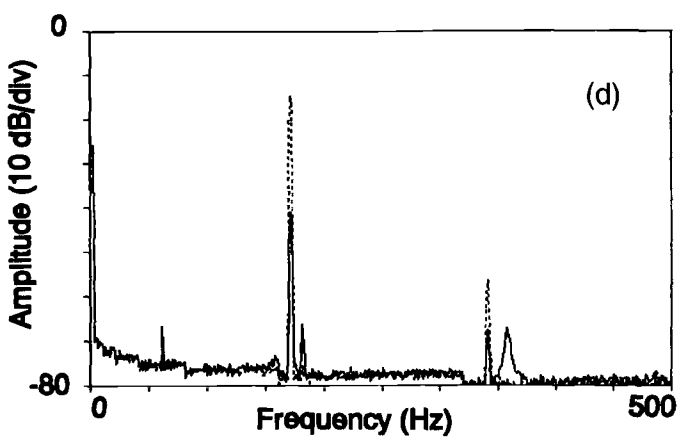
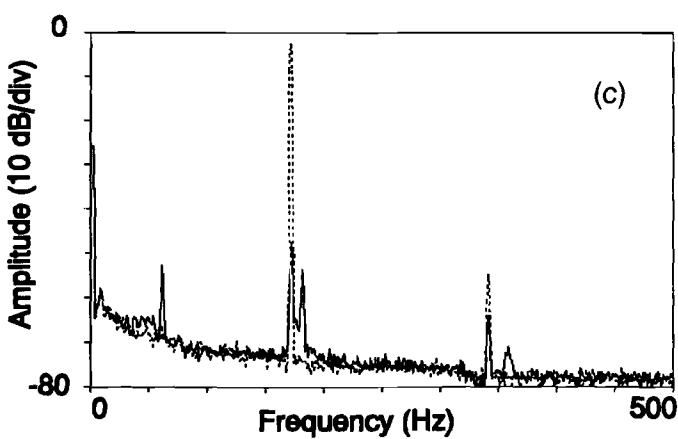
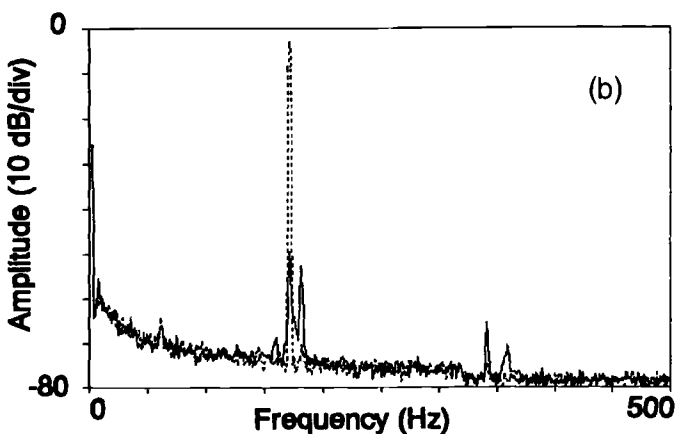
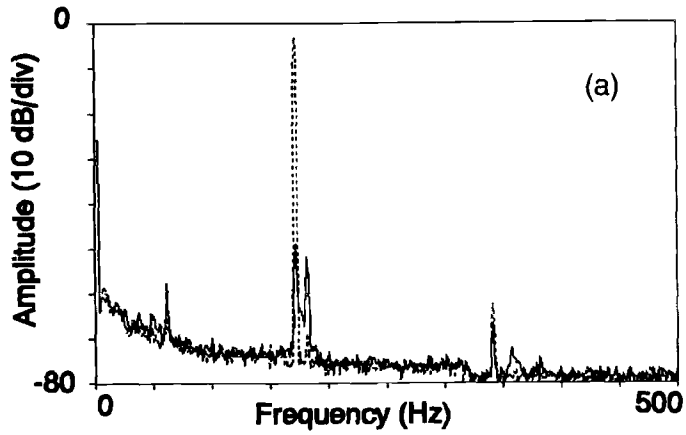


Figure 8. Error signal spectrum for four-channel control. Without control, dashed line; with control, solid line.

(a) corner 1 (c) corner 3
(b) corner 2 (d) corner 4

corner 4. It was found in measuring the vibration level throughout the plate, that the four-channel case resulted in global attenuation of the plate, which was not the case with either the one-channel or two-channel cases.

The previous results were obtained by eliminating feedback from the control system, by using the driving signal for the excitation shaker as the input signal to the adaptive control algorithm. The control system was also tested in the presence of feedback, by employing the fixed compensation filters discussed earlier. The input signal for the control system was obtained from an additional PCB 303A11 accelerometer mounted on the plate approximately 1 cm from the primary excitation point. The results were found to parallel the results obtained for no feedback, which implies that the compensation filters were able to remove the feedback sufficiently well so as not to degrade the performance of the control system. One case is shown in Figure 9 for the case of two-channel control. A

comparison with Fig. 7 shows the differences in control to be minimal. This result was found to be general, in that the results obtained with feedback were very similar to the results obtained without feedback. Thus, the results shown in this paper for the case with no feedback in the system can also be regarded as typical for the case with feedback.

The adaptive control system was also tested using an excitation signal consisting of several frequency components which were input to a single excitation shaker. Figures 10 and 11 show results obtained for two-channel and four-channel control, respectively. In both cases, the input excitation consisted of two sine waves with frequencies of 170 Hz and 381 Hz, corresponding to the (3,1) and (1,3) bending modes of the plate. No feedback was present for the results shown here. The results for multiple frequency excitation are very similar to the previous cases of single frequency excitation. For two-channel control, the vibration at corners 1 and 3 was attenuated very signif-

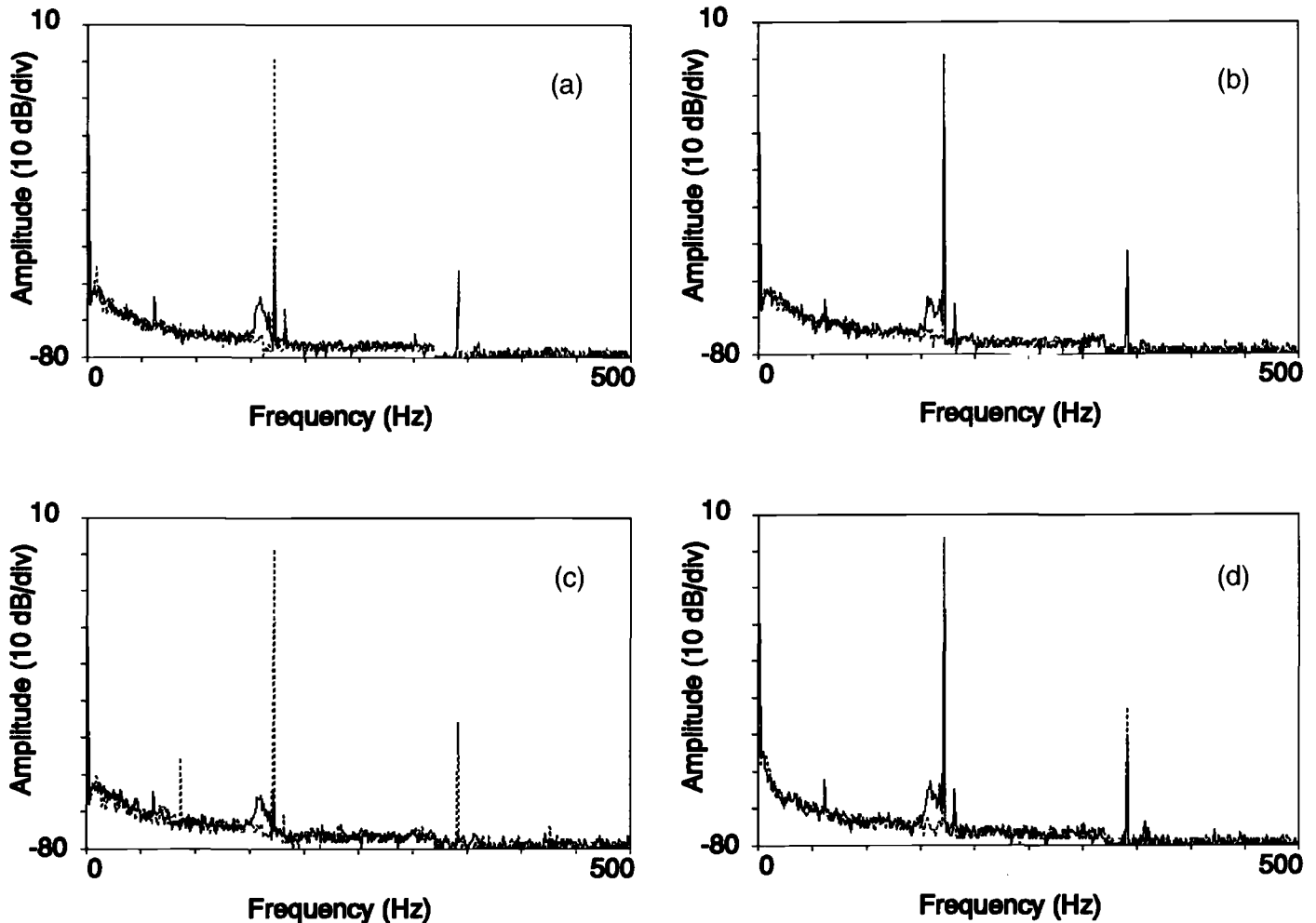


Figure 9. Error signal spectrum for two-channel control with feedback compensation. Without control, dashed line; with control, solid line. Compare with Fig. 7, which is two-channel control without any feedback.

(a) corner 1
(b) corner 2

(c) corner 3
(d) corner 4

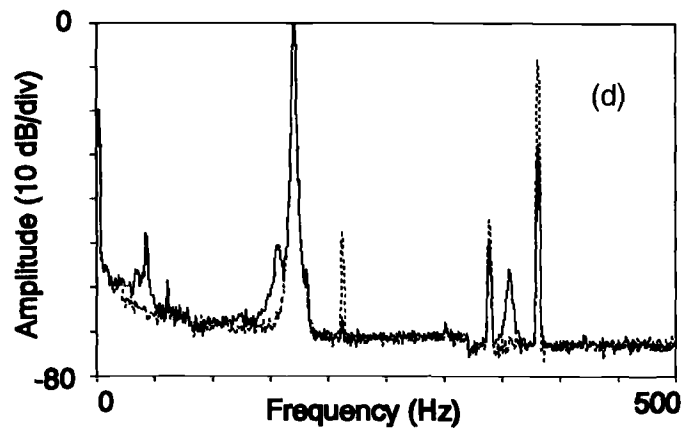
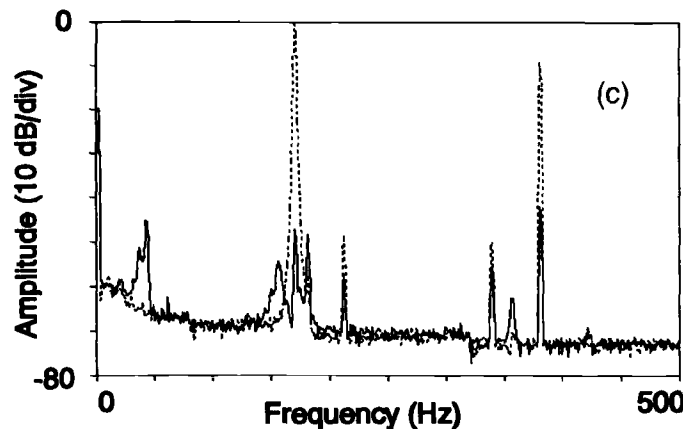
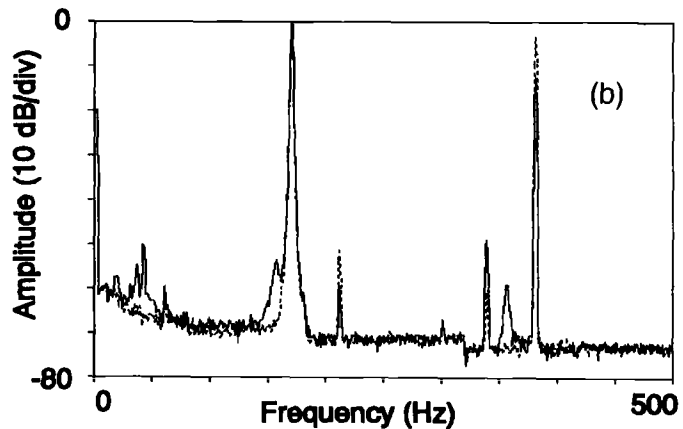
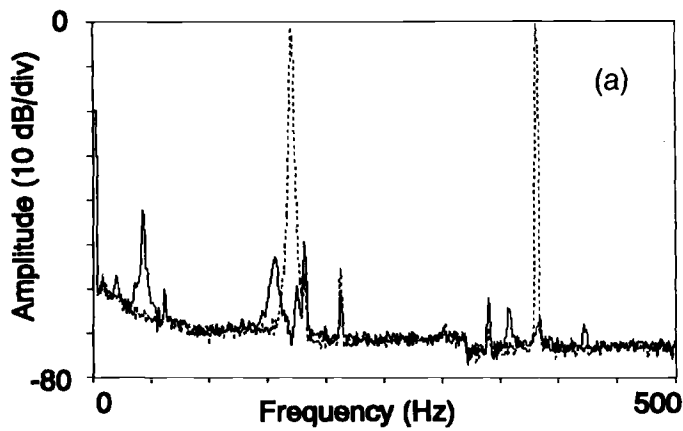


Figure 10. Error signal spectrum for two-channel control with multiple frequency excitation. Without control, dashed line; with control, solid line.

(a) corner 1
(b) corner 2

(c) corner 3
(d) corner 4

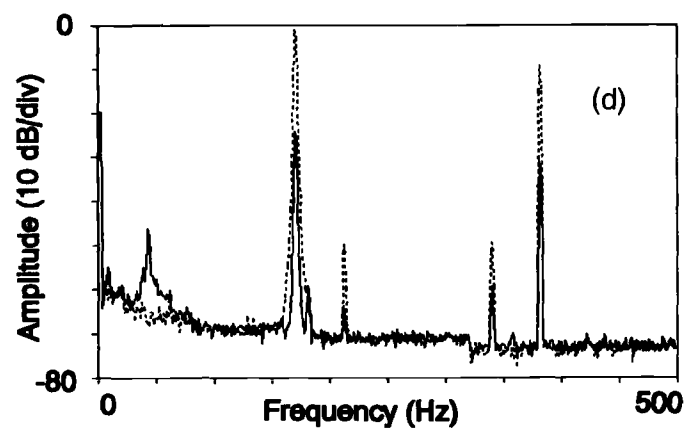
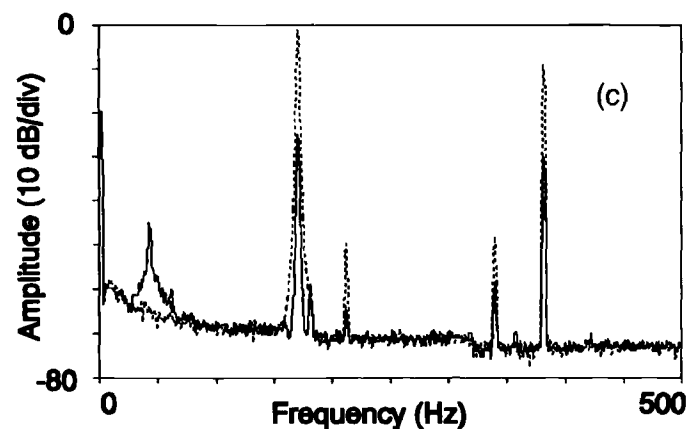
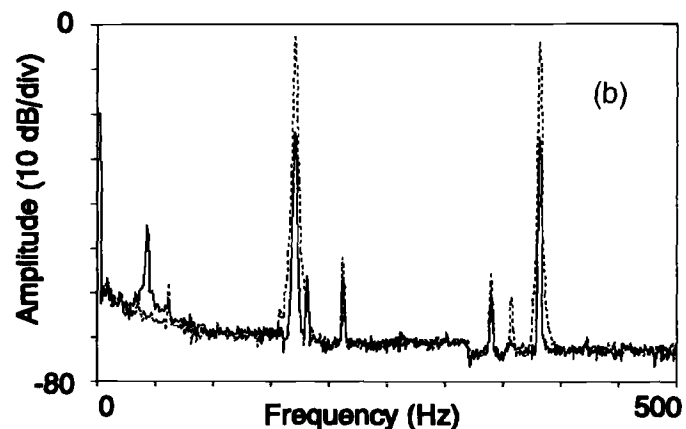
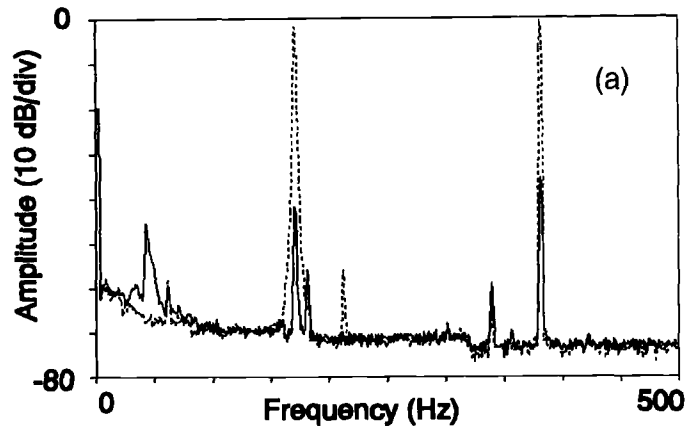


Figure 11. Error signal spectrum for four-channel control with multiple frequency excitation. Without control, dashed line; with control, solid line.

(a) corner 1
(b) corner 2

(c) corner 3
(d) corner 4

icantly at the two excitation frequencies, while the vibration at those frequencies was not attenuated significantly at the two uncontrolled corners. Similarly, for four-channel control, both frequency components were attenuated by at least 20 dB at all four corners of the plate.

The controller has been applied to a number of multiple frequency signals, and demonstrates similar control capability. As long as there is a sufficient number of coefficients in the control filter (a minimum of two per frequency component to be controlled), similar control results can be obtained. For the case of random excitation, the physical nature of the system to be controlled is of utmost importance. For an LMS-based control system, there must be a significant correlation between the input signal to the controller and the signal to be attenuated. For random excitation of structures, this correlation may often be lacking, resulting in poor control of the vibration. Further discussion of this can be found in Ref. 17.

Conclusions

A multi-channel generalization of the filtered-x LMS algorithm has been developed for active control of structural vibration. The system effectively performs both system identification and control in real-time using two parallel adaptive algorithms. Work is currently being done to more completely characterize the nature of the interaction between the two algorithms, as well as more fully developing the stability characteristics of the control system. The application of the control system on a flexible plate has demonstrated that the control system is robust and effective in minimizing the chosen performance function. For the results presented here, the performance function consisted of the sum of the squared error sensor signals at a discrete number of points. The results show that the controller minimizes the vibration at those points, but may not necessarily result in global attenuation of the vibration field.

The case of four-channel control, with control actuators and error sensors located near all four corners generally resulted in global attenuation. However, in general, if global attenuation is desired, attention should be given to selecting the performance function in such a manner that minimizing the performance function also produces the desired global attenuation. Finally, although not shown here, the adaptive controller has also demonstrated the ability to track changing input excitations and changing system parameters. The adaptive control system is currently being used to gain a better understanding of the physical mechanisms involved in multi-channel active control of structures, by means of investigating the modal structure of the plate both without and with control.

Acknowledgment

The author would like to acknowledge the assistance of Mr. Lance B. Bischoff in obtaining the experimental results presented in this paper.

This appendix contains a derivation of the convergence result given in Eq. (24), which is reproduced here for reference.

$$0 < \mu < \frac{2}{h_{\max}^2 [L \cdot M \cdot I \cdot J^2] R_{xx}(0)} . \quad (A1)$$

The range of stable values for μ is given by $0 < \mu < 2/\lambda_{\max}$, where λ_{\max} is the largest eigenvalue of the filtered autocorrelation matrix.²⁶ To arrive at the desired expression, the value of λ_{\max} must be expressed in terms of the average input power. Since the autocorrelation matrix, $E\{\mathbf{R}(n)\mathbf{R}^T(n)\}$, is positive definite, the following relationship exists:

$$\lambda_{\max} \leq \text{trace} [E\{\mathbf{R}(n)\mathbf{R}^T(n)\}] . \quad (A2)$$

Using Eqs. (19) and (15), this can be expressed as

$$\lambda_{\max} \leq \text{trace} \left[E \left\{ \sum_{l=1}^L \mathbf{r}_l(n) \mathbf{r}_l^T(n) \right\} \right] \quad (A3)$$

$$= E \left\{ \sum_{l=1}^L \sum_{m=1}^M \sum_{i=0}^{I-1} r_{lm}^2(n-i) \right\} .$$

Remembering the definition of $r_{lm}(n-i)$ given in Eq. (13) allows Eq. (A3) to be expressed as

$$\begin{aligned} \lambda_{\max} &\leq E \left\{ \sum_{l=1}^L \sum_{m=1}^M \sum_{i=0}^{I-1} \left(\sum_{j=0}^{J-1} h_{lmj}(n)x(n-j-i) \right) \left(\sum_{k=0}^{J-1} h_{lmk}(n)x(n-k-i) \right) \right\} \dots \\ &= \sum_{l=1}^L \sum_{m=1}^M \sum_{i=0}^{I-1} \sum_{j=0}^{J-1} \sum_{k=0}^{J-1} h_{lmj}(n)h_{lmk}(n)E\{x(n-j-i)x(n-k-i)\} , \end{aligned} \quad (A4)$$

where the independence of $h_{lmj}(n)$ and $x(n)$ has been used and $E\{h_{lmj}(n)h_{lmk}(n)\} = h_{lmj}(n)h_{lmk}(n)$. Assuming that $x(n)$ is a stationary process,

$$E\{x(n-j-i)x(n-k-i)\} = R_{xx}(j-k) , \quad (A5)$$

where $R_{xx}(\tau)$ is the autocorrelation function of the input signal, $x(n)$. However, since $R_{xx}(\tau)$ is the input signal autocorrelation function, the maximum value occurs for $\tau = 0$, which corresponds to the average input signal power. Thus, from Eqs. (A4) and (A5),

$$\lambda_{\max} \leq \sum_{l=1}^L \sum_{m=1}^M \sum_{i=0}^{I-1} \sum_{j=0}^{J-1} \sum_{k=0}^{J-1} h_{lmj}(n)h_{lmk}(n)R_{xx}(0) . \quad (A6)$$

Finally, if an upper bound is known for $h_{lmj}(n)$, denoted by h_{\max} , the transfer function coefficients may be removed from the sum to yield

$$\lambda_{\max} \leq h_{\max}^2 \sum_{l=1}^L \sum_{m=1}^M \sum_{i=0}^{l-1} \sum_{j=0}^{l-1} R_{xx}(0), \quad (\text{A7})$$

or

$$\lambda_{\max} \leq h_{\max}^2 [L \cdot M \cdot I \cdot J^2] R_{xx}(0). \quad (\text{A8})$$

The Motorola DSP56000ADS signal processing board which was used is a fixed point processor so that h_{\max} was known to be bounded by a value of 1. Replacing λ_{\max} in the upper bound for the convergence parameter by the expression in Eq. (A8) leads to Eq. (24).

References

1. P.A. Nelson, A.R.D. Curtis, and S.J. Elliott, "On the Active Absorption of Sound," *Proceedings of the International Conference on Noise Control Engineering*, R. Lotz, Ed. (Institute of Noise Control Engineering, Poughkeepsie, NY, 1986), Vol. 1, pp. 601-606.
2. J. Tichy, G.E. Warnaka, and L.A. Poole, "A Study of Active Control of Noise in Ducts," *Journal of Vibration, Acoustics, Stress, and Reliability in Design*, **106**, 399-404 (1984).
3. L.J. Eriksson, M.C. Allie, and R.A. Greiner, "The Selection and Application of an IIR Adaptive Filter For Use in Active Sound Attenuation," *IEEE Transactions on Acoustics, Speech, and Signal Processing*, **ASSP-35**, 433-437 (1987).
4. P.A. Nelson, A.R.D. Curtis, S.J. Elliott, and A.J. Bullmore, "The Active Minimisation of Harmonic Enclosed Sound Fields, Parts I-III," *Journal of Sound and Vibration*, **117**, 1-58 (1987).
5. J.V. Warner, D.E. Waters, and R.J. Bernhard, "Adaptive Active Noise Control in Three Dimensional Enclosures," *Proceedings of the 1988 National Conference on Noise Control Engineering*, M. Bockhoff, Ed. (Noise Control Foundation, New York, NY, 1988), Vol. 1, pp. 285-290.
6. C.A. Rogers, C.R. Fuller, and C. Liang, "Active Control of Sound Radiation From Panels Using Embedded Shape Memory Alloy Fibers," *Journal of Sound and Vibration*, **136**, 164-170 (1990).
7. Jie Pan, C.H. Hansen, and D.A. Bies, "Active Control of Noise Transmission Through a Panel Into a Cavity: I. Analytical Study," *Journal of the Acoustical Society of America*, **87**, 2098-2108 (1990).
8. L. Meirovitch and H. Baruh, "Optimal Control of Damped Flexible Gyroscopic Systems," *Journal of Guidance and Control*, **4**, 157-163 (1981).
9. J.S. Burdess and A.V. Metcalfe, "The Active Control of Forced Vibration Produced by Arbitrary Disturbances," *Journal of Vibration, Acoustics, Stress, and Reliability in Design*, **107**, 33-37 (1985).
10. S. Lee and A. Sinha, "Design of an Active Vibration Absorber," *Journal of Sound and Vibration*, **109**, 347-352 (1986).
11. R.G. Owen and D.I. Jones, "Multivariable Control of an Active Anti-Vibration Platform," *IEEE Transactions on Magnetics*, **MAG-22**, 523-525 (1986).
12. E. Anton and H. Ulbrich, "Active Control of Vibrations in the Case of Asymmetrical High-Speed Rotors by Using Magnetic Bearings," *Journal of Vibration, Acoustics, Stress, and Reliability in Design*, **107**, 410-415 (1985).
13. T. Bailey and J.E. Hubbard Jr., "Disturbed Piezoelectric-Polymer Active Vibration Control of a Cantilever Beam," *Journal of Guidance and Control*, **8**, 605-611 (1985).
14. A.D. White and D.G. Cooper, "An Adaptive Controller for Multivariable Active Noise Control," *Applied Acoustics*, **17**, 99-109 (1984).
15. P.A. Nelson, M.D. Jenkins, and S.J. Elliott, "Active Isolation of Periodic Vibrations," *Proceedings of the 1987 National Conference on Noise Control Engineering*, J. Tichy and S. Hayek, Eds. (Noise Control Foundation, New York, NY, 1987), Vol. 1, pp. 425-430.
16. R.L. Clark and C.R. Fuller, "Active Structural Acoustic Control with Adaptive Structures Including Wavenumber Considerations," *Proceedings of the Conference on Recent Advances in Active Control of Sound and Vibration*, Blacksburg, VA (April 1991).
17. S.D. Sommerfeldt and J. Tichy, "Adaptive Control of a Two-Stage Vibration Isolation Mount," *Journal of the Acoustical Society of America*, **88**, 938-944 (1990).
18. B. Widrow, J.R. Glover, Jr., J.M. McCool, J. Kaunitz, C.S. Williams, R.J. Hearn, J.R. Zeidler, E. Dong, Jr., and R.C. Goodlin, "Adaptive Noise Cancelling: Principles and Applications," *Proceedings of the IEEE*, **63**, 1692-1716 (1975).
19. B. Widrow and S.D. Stearns, *Adaptive Signal Processing* (Prentice-Hall, Englewood Cliffs, NJ, 1985), pp. 99-116.
20. G.C. Goodwin and K.S. Sin, *Adaptive Filtering Prediction and Control* (Prentice-Hall, Englewood Cliffs, NJ, 1984), pp. 50-57.
21. G.C. Goodwin and K.S. Sin, *Adaptive Filtering Prediction and Control* (Prentice-Hall, Englewood Cliffs, NJ, 1984), pp. 68-74.
22. G.E. Warnaka, L.A. Poole, and J. Tichy, "Active Acoustic Attenuator," *United States Patent*, No. 4,473,906, issued: Sept. 25, 1984.
23. L.J. Eriksson, "Active Attenuation System With On-Line Modeling of Speaker, Error Path and Feedback Path," *United States Patent*, No. 4,677,676, issued: June 30, 1987.
24. S.J. Elliott, I.M. Stothers, and P.A. Nelson, "A Multiple Error LMS Algorithm and Its Application to the Active Control of Sound and Vibration," *IEEE Transactions on Acoustics, Speech, and Signal Processing*, Vol. ASSP-35, No. 10 (1987), pp. 1423-1434.
25. B. Widrow and S.D. Stearns, *Adaptive Signal Processing* (Prentice-Hall, Englewood Cliffs, NJ, 1985), pp. 288-294.
26. S.D. Sommerfeldt, "Adaptive Vibration Control of Vibration Isolation Mounts, Using an LMS-Based Control Algorithm," Ph.D. Thesis, The Pennsylvania State University, University Park, PA, 84-86 (1989).
27. S.D. Sommerfeldt, "Adaptive Vibration Control of Vibration Isolation Mounts, Using an LMS-Based Control Algorithm," Ph.D. Thesis, The Pennsylvania State University, University Park, PA, 86-89 (1989).
28. B. Widrow and S.D. Stearns, *Adaptive Signal Processing* (Prentice-Hall, Englewood Cliffs, NJ, 1985), pp. 82-87.
29. G.C. Goodwin and K.S. Sin, *Adaptive Filtering Prediction and Control* (Prentice-Hall, Englewood Cliffs, NJ, 1984), pp. 438-442.